

Investigation of Validation Method for Twisted Hydrofoils in Cavitating Flow

Sinem ÖKSÜZ^{1,*}, Onur USTA² and Fahri ÇELİK¹

¹ Department of Naval Architecture and Marine Engineering, Faculty of Naval Architecture and Maritime, Yildiz Technical University, 34349, Istanbul, Türkiye.

² Department of Naval Architecture and Marine Engineering, Turkish Naval Academy, National Defence University, 34942, Tuzla, Istanbul, Türkiye

* sinem.oksuz.91@gmail.com

ABSTRACT

This study investigates the cavitating flow around a twisted NACA 0009 hydrofoil using both Reynolds-Averaged Navier-Stokes (RANS) and Detached Eddy Simulation (DES) methods to assess their capabilities in capturing unsteady cavitation phenomena. Numerical results were validated against experimental data provided by Foeth (2008a) under a cavitation number of 1.07 and an angle of attack of -2° . While the RANS method provided accurate predictions for lift and drag coefficients with lower computational cost, it failed to capture the transient nature of cavitation. In contrast, the DES method successfully resolved the periodic cavitation cycles and demonstrated improved capability in visualizing dynamic cavitation behavior. A time step sensitivity analysis was also conducted, revealing that larger time steps enhance the visibility of cavitation cycles but may lead to overprediction of the cavitation region. Overall, the findings highlight that although RANS is sufficient for hydrodynamic performance evaluation, DES is more suitable for analyzing unsteady cavitation dynamics around hydrofoils.

Keywords: Cavitation, Twisted, Hydrofoil, RANS, DES

1 INTRODUCTION

Hydrofoils are widely used in marine applications such as ship rudders, propellers, turbines, and control surfaces due to their capability to generate lift and control manoeuvrability. Among the various hydrofoil designs, twisted hydrofoils offer advantages in achieving efficient lift distribution, drag reduction, and improved flow stability across a range of operating conditions (Liu et al., 2006; Kim et al., 2014). These advantages make twisted hydrofoils an active research subject, particularly under cavitating flow conditions where complex unsteady phenomena occur.

Cavitation, characterized by the formation and collapse of vapor cavities, presents significant challenges to marine hydrodynamic components. It can cause surface erosion, vibration, loss of efficiency, and structural damage (Usta and Korkut, 2019). Accurately capturing cavitation dynamics around twisted hydrofoils requires advanced modeling approaches capable of resolving transient flow structures.

Numerical methods based on the Reynolds-Averaged Navier-Stokes (RANS) equations are commonly used due to their computational efficiency and reasonable accuracy for steady-state performance predictions. However, RANS methods tend to underpredict unsteady phenomena such as cavity shedding and transient pressure fluctuations (Köksal et al., 2021). To address these limitations, hybrid turbulence modeling techniques

like Detached Eddy Simulation (DES) have been introduced. DES offers improved resolution of time-dependent cavitation structures by combining RANS modeling in the boundary layer with Large Eddy Simulation (LES) in separated regions (Shur et al., 2008; Gritskevich et al., 2012).

Recent studies highlight the importance of mesh resolution and time step sensitivity in cavitation simulations. Capturing periodic cavitation structures and vapor shedding cycles requires not only appropriate turbulence models but also carefully selected numerical parameters (Melissaris et al., 2019; Yin et al., 2021).

This study aims to investigate the cavitating flow around a twisted NACA0009 hydrofoil by comparing the performance of RANS and DES approaches in terms of accuracy and capability to capture cavitation dynamics. The validation is conducted using experimental data from the Delft Twisted 11 Hydrofoil (Foeth, 2008a). Additionally, the effect of time step size on the accurate prediction of cavitation cycles is analysed. The results are expected to provide insights into the numerical modelling of unsteady cavitating flows and support the selection of appropriate CFD strategies for hydrofoil simulations.

2 NUMERICAL MODELLING

In the analyses, the Detached Eddy Simulation method was used, which applies Reynolds Averaged Navier Stokes modelling in the region near the wall and direct solution in the regions far from the wall. To model the cavitation, the Schnerr-Sauer model was used, which provides a numerical solution assuming that the cavitation bubbles have the same radius and properties.

2.1 Reynolds Averaged Navier Stokes (RANS)

The RANS method is the modeling of turbulent flow by time averaging the Navier Stokes equations. The flow velocity is defined as two components as it given below:

$$u = u' + \bar{u} \quad (1)$$

The time averaged Navier Stokes equation can be written as;

$$\overline{\overline{u} \cdot \nabla u} = \frac{-1}{\rho} \nabla \bar{p} + \mu \nabla^2 \bar{u} + RANS \text{ terms} \quad (2)$$

The Reynolds stress tensor is defined as:

$$\overline{\overline{u' u'}} = \mu t (\nabla \bar{u} + \nabla \bar{u}^T) - \frac{2}{3} k I \quad (3)$$

I is identity matrix, u' is fluctuating velocity and \bar{u} is mean velocity in the formulas.

2.2 Detached Eddy Simulation (DES)

The Detached Eddy Simulation (DES) method is used to solve flow region in the simulations. In this section, only the governing equations employed in the DES method are presented. For a more comprehensive explanation and detailed formulation, the reader is referred to Usta et al. (2025).

$$\frac{\partial u}{\partial t} + u \cdot \nabla u = -\frac{1}{\rho} \nabla p + \mu \nabla^2 u + S \quad (4)$$

$$S = \tau_{SGS} - \frac{2}{3} \text{tr}(\tau_{SGS})I \quad (5)$$

$$\beta = \frac{1}{1 + \left(\frac{L_{DES}}{L_{LES}}\right)^f} \quad (6)$$

The u indicates flow velocity, p is pressure, μ is dynamic viscosity, τ_{SGS} is stress tensor, β is mixing function, L_{DES} and L_{LES} are turbulence length scales and f is a transition control parameter.

2.3 Schnerr-Sauer Cavitation Model

The Schnerr-Sauer cavitation model assumes that the cavitation bubbles are round and have the same radius. In this method, the bubble radius (R_{bubble}) is given by the following formula:

$$R_{bubble} = \left(\frac{\alpha_v}{1 - \alpha_v} \cdot \frac{3}{4\pi} \cdot \frac{1}{n_{bubble}} \right)^{1/3} \quad (7)$$

In the formulation, α_v is vapour volume fraction and n_{bubble} is the number of bubbles per unit volume of liquid. For further information about the Schnerr-Sauer cavitation model, please see Usta and Korkut, (2019).

2.4 Numerical Setup and Mesh Generation

The simulations were performed under cavitating flow conditions. The inlet velocity was set to 6.97 m/s and the outlet pressure to 29 kPa, resulting in a cavitation number (σ) of 1.07. Water and vapor phases were modelled as a homogeneous mixture, and the Schnerr-Sauer cavitation model was employed for phase change predictions. All simulations were carried out using STAR-CCM. The analyse conditions given in the table below.

Table 1: Physical conditions for the simulations

Method	Reynolds Averaged Navier Stokes	Detached Eddy Simulation
Turbulence model	k-omega	k-omega
Cavitation model	Schnerr-Sauer	Schnerr-Sauer
Flow velocity	6.97 m/s	6.97 m/s
Cavitation number	1.07	1.07
Outlet pressure	29 kPa	29 kPa
Saturation pressure	2970 Pa	2970 Pa
Time step	10^{-5}	$10^{-5}, 2 \times 10^{-5}$

Turbulence was modelled using the SST k- ω model for both RANS and DES simulations. DES was employed enabling scale-resolving behaviour in separated flow regions. The unstructured hexahedral mesh used for RANS simulations consisted of approximately 4.5 million elements, while DES simulations used a refined mesh with about 12 million elements to ensure sufficient resolution in the separated and cavitating regions. The Courant number was kept below 1 to satisfy numerical stability criteria.

3 METHODOLOGY

3.1 Computational Domain and Boundary Conditions

The simulations were carried out using the twisted NACA0009 hydrofoil geometry based on the Delft Twisted 11 configuration, with a span of 0.3 m and a chord length of 0.15 m. The hydrofoil was placed in a 3D

computational domain designed to replicate the conditions of the cavitation tunnel experiments conducted by Foeth (2008a). To minimize boundary effects and accurately capture the flow, the inlet and outlet boundaries were positioned at distances of $2c$ and $5c$ from the hydrofoil's leading and trailing edges, respectively, while one chord length spacing was maintained from the top and bottom walls.

A symmetry plane was applied along the spanwise mid-plane to reduce computational cost. A velocity inlet and pressure outlet boundary condition were defined, with slip walls assigned to domain boundaries and a no-slip condition applied on the hydrofoil surface.

The computational domain and hydrofoil can be seen in the Figure 1 below.

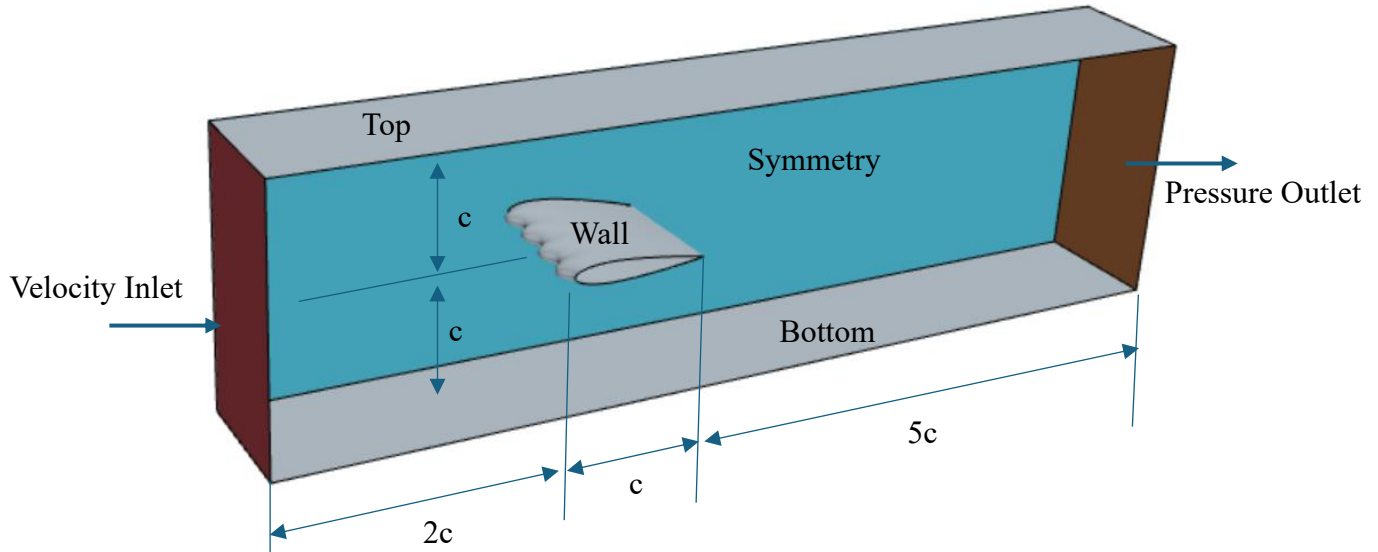


Figure 1: Computational domain and hydrofoil

3.2 RANS and DES Comparison for Cavitating Flow

Figure 2 presents the comparison of cavitation volume over time obtained from RANS and DES simulations at the same mesh density and time step ($\Delta t = 1 \times 10^{-5}$ s). The RANS solution exhibits a nearly steady cavitation volume after initial transients, indicating a quasi-steady behaviour. In contrast, the DES simulation captures periodic oscillations in cavitation volume, corresponding to cavity shedding events, closely matching experimental observations.

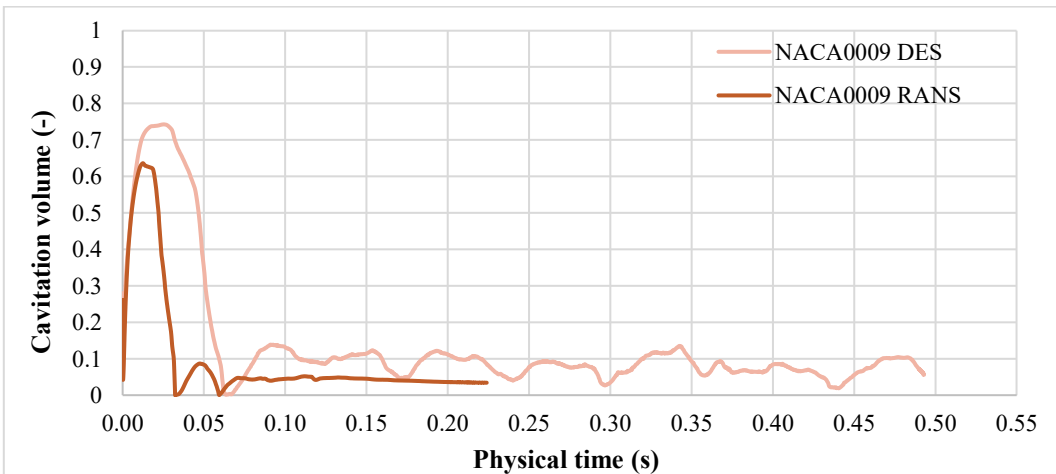


Figure 2. Cavitation development by time for NACA0009 Twisted at $\text{AoA} = -2^\circ$ (RANS and DES).

These results confirm that while RANS is sufficient for estimating average lift and drag coefficients, it fails to resolve the unsteady nature of cavitation. DES, by capturing periodic cavity dynamics, offers a more realistic depiction of the physical phenomenon.

Table 2: Comparison of the drag and lift coefficients obtained in the present study with those reported in the literature

	Foeth (2008b) (Experiment)	(Whitworth, 2011) RANS	(Usta, 2018) DES	Present study RANS	Present study DES
C_D	-	0.0242	0.0266	0.0236	0.0401
C_L	0.523	0.403	0.433	0.428	0.443

3.3 Time Step Sensitivity in DES Simulations

To evaluate the influence of time step on the accuracy of unsteady cavitation predictions, additional DES simulations were performed with $\Delta t = 2 \times 10^{-5}$ s. As shown in Figure 3 and Table 3, increasing the time step resulted in an overestimation of the cavitation volume and a longer cavitation cycle period. The average lift coefficient also decreased with the larger time step, while drag values remained similar.

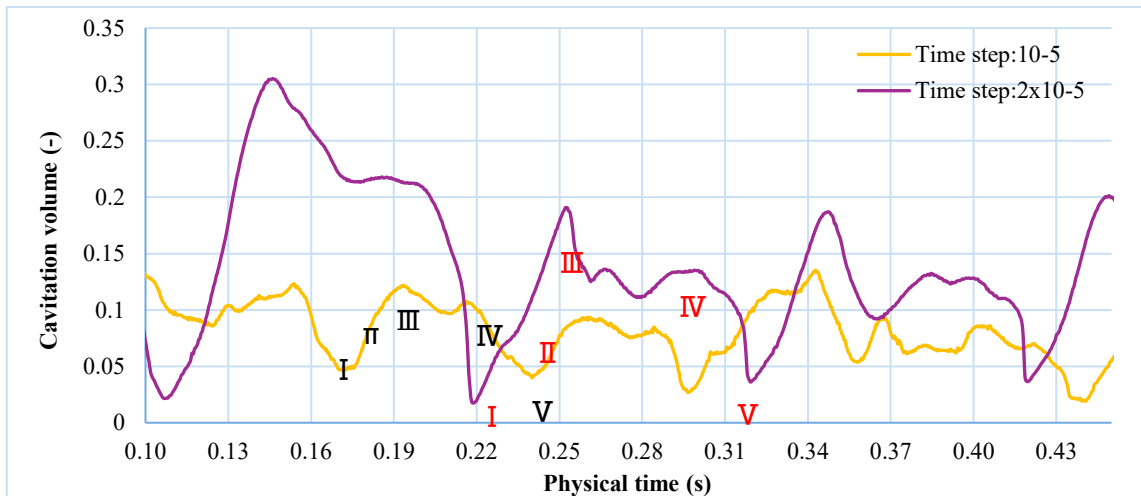


Figure 3: Cavitation volume curves for time step $\Delta t=1 \times 10^{-5}$ s and $\Delta t=2 \times 10^{-5}$ s.

Table 3: Cavitation development by time on the NACA0009 Twisted hydrofoil.

Twisted NACA0009 AoA= -2°	I T=0	II T/4	III T/2	IV 3T/4	V T
Experiment (Foeth,2008a)					
Present Study DES Time Step: 1×10^{-5}					
Present Study DES Time Step: 2×10^{-5}					

These results indicate that accurate resolution of cavitation shedding, and force fluctuations requires a sufficiently small-time step. Based on the findings, a time step of $\Delta t = 1 \times 10^{-5}$ s provides a good balance between accuracy and computational cost for capturing cavitation cycles in DES.

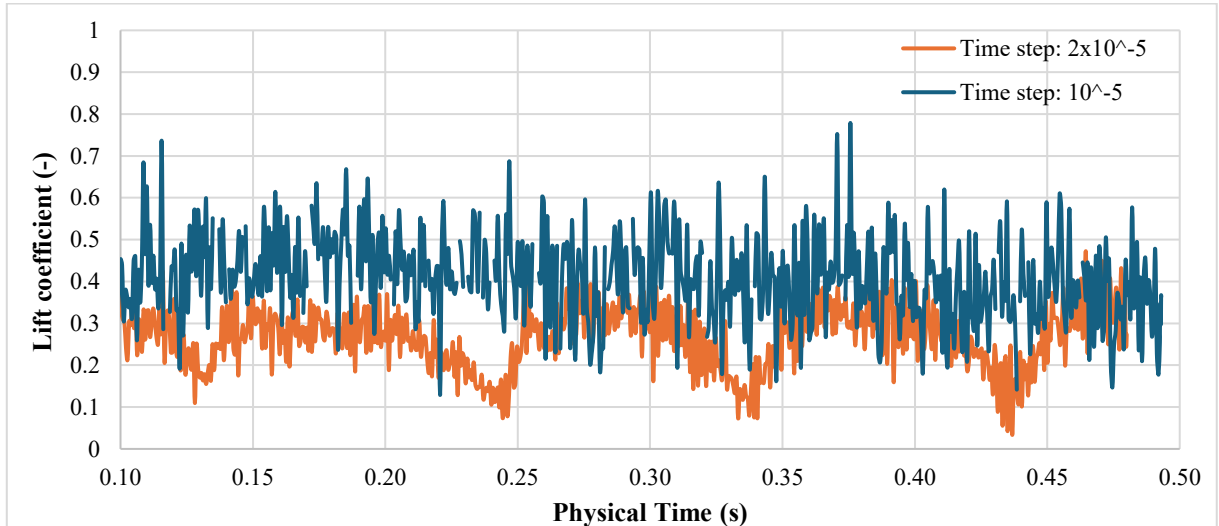


Figure 4: Lift force coefficient curves for the NACA0009 twisted hydrofoil with $\text{AoA} = -2^\circ$, with two different time step values, $\Delta t = 10^{-5}$ s and $\Delta t = 2 \times 10^{-5}$ s.

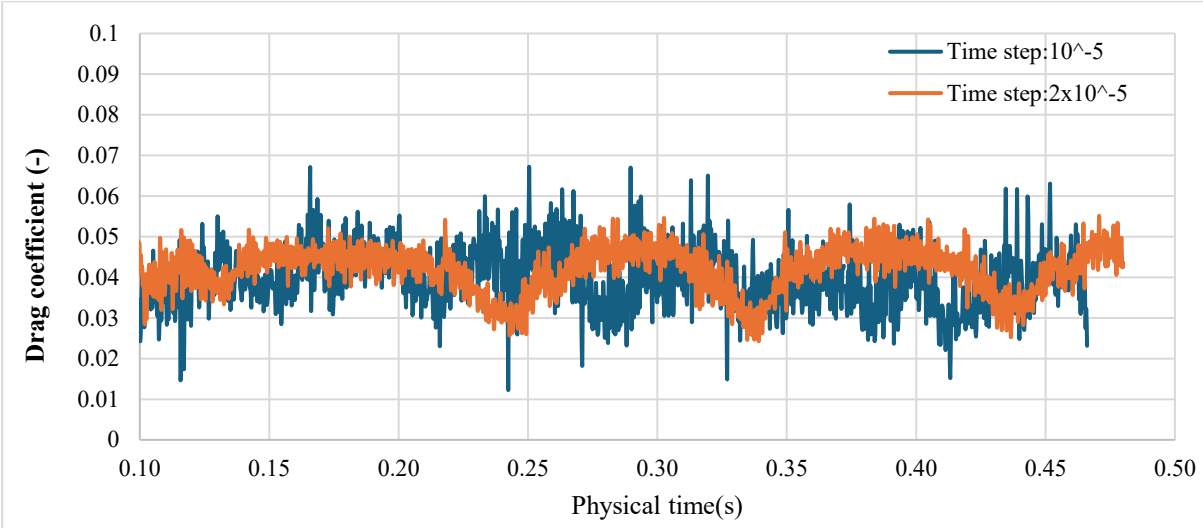


Figure 5: Drag force coefficient curves for the NACA0009 twisted hydrofoil with $\text{AoA} = -2^\circ$, with two different time step values, $\Delta t = 10^{-5}$ s and $\Delta t = 2 \times 10^{-5}$ s.

The results confirmed the accuracy of the solution for a time step of $\Delta t = 10^{-5}$ s. However, the cavitation cycle characteristics during this period appear to be roughly similar across different time steps. Moreover, the lift and drag coefficient graphs in Figures 4 and 5 indicate that the timing of cavitation formation aligns with the patterns shown in these figures. While the average drag coefficient remains nearly constant at around $C_D = 0.04$ for different time intervals, the average lift coefficient shows a slight decrease as the time step increases ($C_L = 0.443$ for $\Delta t = 10^{-5}$ s and $C_L = 0.28$ for $\Delta t = 2 \times 10^{-5}$ s).

4 RESULTS & DISCUSSION

The RANS and DES methods were employed to simulate cavitating flow around the twisted NACA 0009 hydrofoil, and their results were compared with the experimental data presented by Foeth (2008a). The simulations were conducted under a cavitation number of 1.07 and an angle of attack of -2° , replicating the experimental setup for validation purposes.

Initially, the RANS method was used due to its lower computational cost. The simulations showed that the cavitation region over the hydrofoil stabilizes after a certain time, preventing the capture of unsteady cavitation phenomena. However, the computed lift and drag coefficients were in good agreement with both experimental and numerical results reported in the literature, indicating that RANS is sufficient for evaluating overall hydrodynamic performance.

Subsequently, the DES method was applied under the same physical conditions to investigate the dynamic behavior of cavitation. In contrast to RANS, the DES approach successfully captured periodic cavitation cycles, allowing for an accurate estimation of cavitation periods. The calculated lift and drag coefficients were also found to be consistent with those obtained using RANS, further supporting the reliability of the DES method.

In summary, while the RANS method is suitable for predicting hydrodynamic performance, it falls short in capturing unsteady cavitation behavior, particularly at lower angles of attack. The DES method, with its ability to resolve transient flow structures, is more appropriate for investigating periodic cavitation formation.

In the subsequent analysis, the effect of time step size was examined by comparing numerical results with high-speed camera images from Foeth's (2008) experimental study. At a larger time step ($\Delta t = 2 \times 10^{-5}$ s), cavitation cycles appeared more clearly; however, the extent of the cavitation region over the hydrofoil was

overpredicted. Reducing the time step led to more accurate representation of the cavitation area and improved agreement with experimental observations.

5 REFERENCES

Foeth, E.J. (2008a). The structure of three-dimensional sheet cavitation, Delft University of Technology, Department of Marine Technology, PhD Thesis.

Foeth, E.J. (2008b). Pressure and Lift Measurements on Twist-11 Hydrofoil, Delft University of Technology, Report.

Gritskevich, M. S., Garbaruk, A. v., Schütze, J., & Menter, F. R. (2012). Development of DDES and IDDES formulations for the $k-\omega$ shear stress transport model. *Flow, Turbulence and Combustion*, 88(3), 431–449. <https://doi.org/10.1007/S10494-011-9378-4/METRICS> <https://doi.org/10.1016/j.oceaneng.2018.04.064>

Kim, J. H., Choi, J. E., Choi, B. J., & Chung, S. H. (2014). Twisted rudder for reducing fuel-oil consumption. *International Journal of Naval Architecture and Ocean Engineering*, 6(3), 715–722. <https://doi.org/10.2478/IJNAOE-2013-0207>

Köksal, Ç. S., Usta, O., Aktas, B., Atlar, M., & Korkut, E. (2021). Numerical prediction of cavitation erosion to investigate the effect of wake on marine propellers. *Ocean Engineering*, 239, 109820. <https://doi.org/10.1016/J.OCEANENG.2021.109820>

Liu, T., Kuykendoll, K., Rhew, R., & Jones, S. (2006). Avian wing geometry and kinematics. *AIAA Journal*, 44(5), 954–963. <https://doi.org/10.2514/1.16224>

Melissaris, T., Bulten, N., & van Terwisga, T. J. C. (2019). On the applicability of cavitation erosion risk models with a URANS solver. *Journal of Fluids Engineering, Transactions of the ASME*, 141(10). <https://doi.org/10.1115/1.4043169>

Oksuz, S., Celik, F., & Bayraktar, S. (2023). Three-dimensional computational analysis of flow over twisted hydrofoils. *Ocean Engineering*, 267, 113304. <https://doi.org/10.1016/J.OCEANENG.2022.113304>

Shur, M. L., Spalart, P. R., Strelets, M. K., & Travin, A. K. (2008). A hybrid RANS-LES approach with delayed-DES and wall-modelled LES capabilities. *International Journal of Heat and Fluid Flow*, 29(6), 1638–1649. <https://doi.org/10.1016/J.IJHEATFLUIDFLOW.2008.07.001>

Usta, O., & Korkut, E. (2018). A study for cavitating flow analysis using DES model. *Ocean Engineering*, 160, 397–411. <https://doi.org/10.1016/J.OCEANENG.2018.04.064>

Usta, O., & Korkut, E. (2019). Prediction of cavitation development and cavitation erosion on hydrofoils and propellers by Detached Eddy Simulation. *Ocean Engineering*, 191, 106512.

Usta, O., Çelik, F. & Öksüz, S. (2025). Effect of Leading-Edge Tubercles and Surface Corrugations on the Performance and Cavitation Characteristics of Twisted Hydrofoils, *Ocean Engineering*, 335, 121663

Whitworth, S. (2011). Cavitation prediction of flow over the Delft Twist 11 Foil. *Second International Symposium on Marine Propulsors*, 15–17.

Yin, T., Pavesi, G., Pei, J., & Yuan, S. (2021). Numerical investigation of unsteady cavitation around a twisted hydrofoil. *International Journal of Multiphase Flow*, 135. <https://doi.org/10.1016/j.ijmultiphaseflow.2020.103506>